

# Comparison of Micelles Formed by Amphiphilic Star Block Copolymers Prepared in the Presence of a Nonmetallic Monomer Activator

HOON HYUN,<sup>1,2</sup> JAE SONG CHO,<sup>1,2</sup> BYUNG SOO KIM,<sup>1</sup> JUNG WON LEE,<sup>1,2</sup> MOON SUK KIM,<sup>1</sup> GILSON KHANG,<sup>2</sup> KINAM PARK,<sup>3</sup> HAI BANG LEE<sup>1</sup>

<sup>1</sup>Fusion Biotechnology Research Center, Korea Research Institute of Chemical Technology, Yuseong, Daejeon 305-600, Korea

<sup>2</sup>BK-21 Polymer BIN Fusion Research Team, Chonbuk National University, Duckjin, Jeonju 561-756, Korea

<sup>3</sup>Department of Biomedical Engineering and Pharmaceutics, Purdue University, West Lafayette, Indiana 47907-1791

Received 5 June 2007; accepted 13 November 2007

DOI: 10.1002/pola.22543

Published online in Wiley InterScience (www.interscience.wiley.com).

**ABSTRACT:** In this article, we describe the synthesis of PEG-*b*-polyester star block copolymers via ring-opening polymerization (ROP) of ester monomers initiated at the hydroxyl end group of the core poly(ethylene glycol) (PEG) using HCl Et<sub>2</sub>O as a monomer activator. The ROP of  $\epsilon$ -caprolactone (CL), trimethylene carbonate (TMC), or 1,4-dioxan-2-one (DO) was performed to synthesize PEG-*b*-polyester star block copolymers with one, two, four, and eight arms. The PEG-*b*-polyester star block copolymers were obtained in quantitative yield, had molecular weights close to the theoretical values calculated from the molar ratio of ester monomers to PEG, and exhibited monomodal GPC curves. The crystallinity of the PEG-*b*-polyester star block copolymers was determined by differential scanning calorimetry and X-ray diffraction. Copolymers with a higher arm number had a higher tendency toward crystallization. The crystallinity of the PEG-*b*-polyester star block copolymers also depended on the nature of the polyester block. The CMCs of the PEG-*b*-PCL star block copolymers, determined from fluorescence measurements, increased with increasing arm number. The CMCs of the four-arm star block copolymers with different polyester segments increased in the order 4a-PEG-*b*-PCL < 4a-PEG-*b*-PDO < 4a-PEG-*b*-PLGA < 4a-PEG-*b*-PTMC, suggesting a relationship between CMC and star block copolymer crystallinity. The partition equilibrium constant,  $K_v$ , which is an indicator of the hydrophobicity of the micelles of the PEG-polyester star block copolymers in aqueous media, increased with decreasing arm number and increasing crystallinity. A key aspect of the present work is that we successfully prepared PEG-*b*-polyester star block copolymers by a metal-free method. Thus, unlike copolymers synthesized by ROP using a metal as the monomer activator, our copolymers do not contain traces of metals and hence are more suitable for biomedical applications. Moreover, we confirmed that the PEG-*b*-polyester star block copolymers form micelles and hence may be potential hydrophobic drug delivery vehicles. © 2008 Wiley Periodicals, Inc. *J Polym Sci Part A: Polym Chem* 46: 2084–2096, 2008

**Keywords:** biomaterials; micelles; monomer activator; polyester; poly(ethylene glycol); ring-opening polymerization; star block copolymer

## INTRODUCTION

Star polymers have attracted much attention on account of their useful rheological and mechanical

Correspondence to: M. S. Kim (E-mail: mskim@kriect.re.kr)

*Journal of Polymer Science: Part A: Polymer Chemistry*, Vol. 46, 2084–2096 (2008)  
© 2008 Wiley Periodicals, Inc.

properties, and are expected to display diverse morphologies in comparison with conventional linear polymers.<sup>1–3</sup> Star block copolymers with hydrophilic and hydrophobic segments have also attracted much interest because of their microdomain separation feature.<sup>4,5</sup>

Poly(ethylene glycol) (PEG) is a nontoxic and biocompatible material that is widely used in biomedical applications.<sup>6,7</sup> Its good hydrophilicity means that it is easily removed from the body by excretion through urine. Biodegradable polyesters are attractive materials for use as synthetic biomaterials or controlled drug release matrices because of their good biodegradability and biocompatibility. Recently, considerable effort has been devoted in creating biodegradable block copolymers of polyesters and PEG with biocompatible PEG blocks.<sup>8–12</sup>

PEG and polyester star block copolymers are therefore a particularly promising class of materials. By varying their structure, which consists of radially extended arms attached to a central core, they can be used as variable building blocks for structured polymer networks (e.g., hydrogels, micelles, or amphiphilic network systems) for biomedical and pharmaceutical applications.<sup>13–15</sup> Thus, this family of polymers may provide a useful starting point in efforts to improve both the physical properties and controlled drug release profiles of PEG and polyester based materials.

One route for preparing PEG and polyester star block copolymers is via the ring-opening polymerization (ROP) of ester monomers by the hydroxyl end group of PEG.<sup>16–18</sup> This approach has been used to synthesize PEG-*b*-poly(L-lactide) (PLLA) and PEG-*b*-poly( $\epsilon$ -caprolactone) (PCL) star block copolymers by ROP of L-lactide (LA) and  $\epsilon$ -caprolactone (CL), respectively, using PEG as an initiator with stannous or metal catalysts.<sup>18–22</sup> Other polyesters could potentially be synthesized by ROP of ester monomers such as trimethylene carbonate (TMC) and 1,4-dioxan-2-one (DO) to prepare PEG-*b*-polyester star block copolymers with poly(1,4-dioxan-2-one) (PDO), or poly(trimethylene carbonate) (PTMC) as the polyester block.<sup>23–25</sup> These copolymers have the advantage that their degradation does not result in an acid environment, unlike the degradation of PLLA and poly(lactide-*co*-glycolide) (PLGA).

Although ROP using a metal catalyst satisfactorily affords star block copolymers with a polyester block, problems have been identified in the star block copolymers obtained by this synthetic

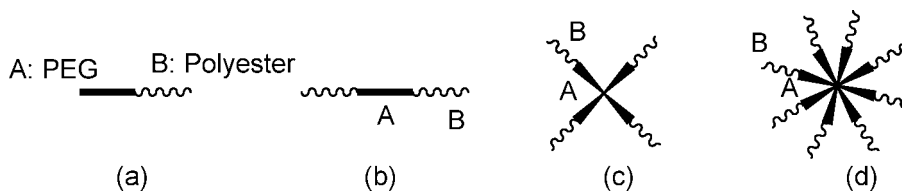
route, in particular the presence of residual metal in the polymer material due to the difficulty of removing the metal catalyst from the polymer matrix.<sup>26</sup> This tendency for metal to remain in the polymer is especially problematic for polymers destined for biomedical and pharmacological applications. Thus, it is desirable to develop a metal-free method for synthesizing PEG and polyester star block copolymers.<sup>27–31</sup> To our knowledge, however, the star block copolymerization of CL, TMC, or DO in the presence of PEG as an initiator has never been performed using HCl as the monomer activator, despite the fact that HCl is a widely available commercial product that is easier to use than metal-based initiators such as stannous octoate.<sup>32,33</sup>

Here, we describe the first synthesis of PEG-*b*-polyester star block copolymers via ROP of CL, TMC, or DO from the hydroxyl end group of core PEG in the presence of HCl Et<sub>2</sub>O as a monomer activator, since we believe this method has a possibility of utilizing a wide range of ester monomers leading to PEG-*b*-polyester star block copolymers with controlled characteristics. To our knowledge, in addition, a little previous study has handled with changes in the number of arms and in the polyester segments for the micelle formation. Thus, we examine the micelle formation behavior of the star block copolymers to understand how the number of arms, and changes in the polyester segments and crystallinity of PEG-*b*-polyester star block copolymers influence the critical micelle concentration (CMC) and partitioning of the hydrophobic molecule pyrene.

## RESULTS AND DISCUSSION

### Preparation of PEG-*b*-polyester Star Block Copolymers

PEG molecules with four or eight terminal alcohols ( $M_n$ , 2000 g/mol) were used as the initiator to prepare four- or eight-arm PEG-*b*-polyester star block copolymers (Scheme 1). MPEG-OH and HO-PEG-OH ( $M_n$ , 2000 g/mol) were used to obtain one- and two-arm block copolymers. One-arm (1a-MPEG-*b*-PCL), two-arm (2a-PCL-*b*-PEG-*b*-PCL), four-arm (4a-PEG-*b*-PCL, 4a-PEG-*b*-PDO, and 4a-PEG-*b*-PTMC), and eight-arm (8a-PEG-*b*-PCL) star block copolymers were synthesized via the ROP of CL, DO, or



Scheme 1

TMC as the monomer using the terminal alcohol of PEG as an initiator in the presence of HCl Et<sub>2</sub>O at room temperature. For comparison, the polymerization of a mixture of LA and glycolide (GA) by PEG was also performed in the presence of stannous octoate to produce a four-arm block copolymer (4a-PEG-*b*-PLGA). In all of the star block copolymers synthesized, the molecular weights of the hydrophobic and hydrophilic segments were designed to have a constant value of 2000 g/mol. In the series of PEG-*b*-PCL star block copolymers, this gives structures in which the hydrophilic and hydrophobic blocks become shorter with increasing arm number.

We were able to prepare large quantities of star block copolymers by using HCl Et<sub>2</sub>O as a monomer activator, and it was easy to purify the star block copolymers after the polymerization. The star block copolymers of PCL, PDO, or PTMC with PEG could be prepared with a controlled molecular weight. Figure 1 shows the <sup>1</sup>H NMR spectra for the four-arm star block copolymers obtained. The star block copolymer exhibited characteristic peaks of polyester as a shell and PEG as a core. The molecular weights can be calculated by integration of the <sup>1</sup>H NMR spectra, that is by calculating the ratio of the ethylene oxide protons of the PEG main chain to the characteristic methylene protons of the poly-

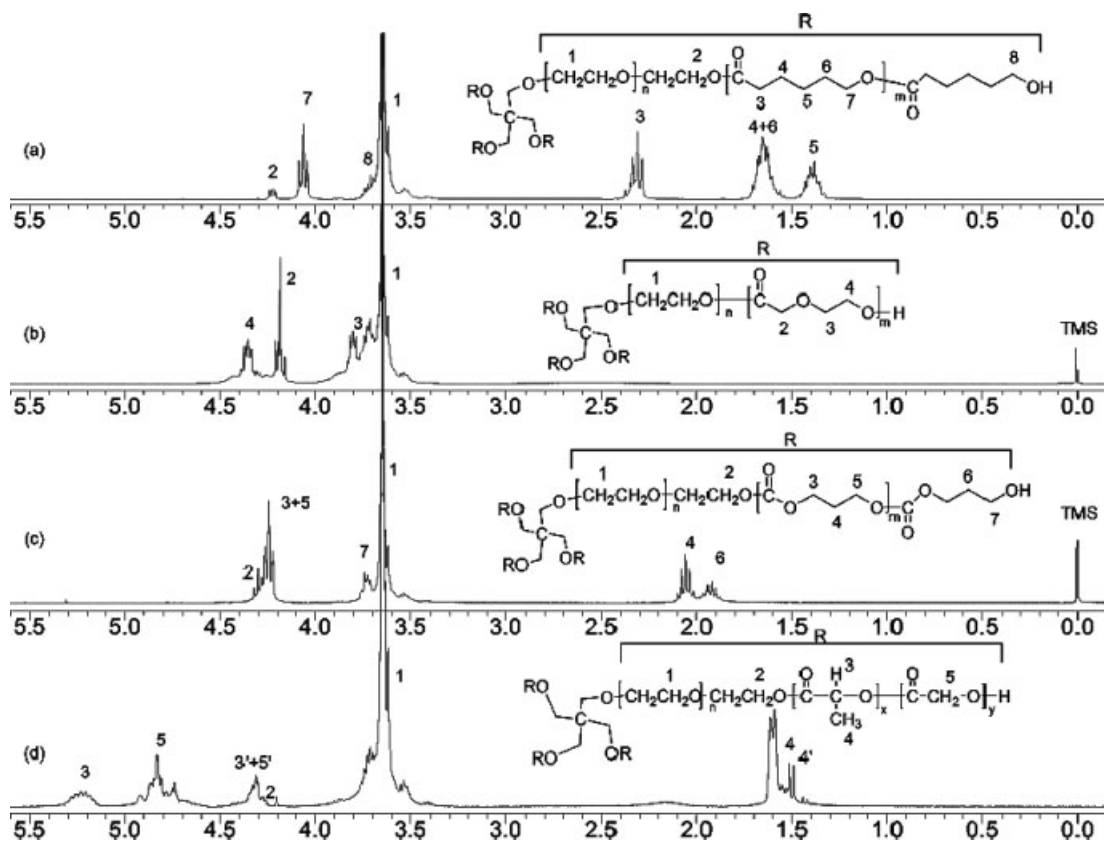


**Figure 1.** <sup>1</sup>H NMR spectra of various four-arm PEG-*b*-polyester star block copolymers in CDCl<sub>3</sub>: (a) 4a-PEG-*b*-PCL, (b) 4a-PEG-*b*-PDO, (c) 4a-PEG-*b*-PTMC, and (d) 4a-PEG-*b*-PLGA.

**Table 1.** Synthesis of PEG-*b*-polyester Star Block Copolymers

Sample	[M]/[I]	$M_{n,calcd}^a$ PEG-polyesters	Yield <sup>b</sup> (%)	$M_{n,GPC}^c$ PEG-polyesters (total $M_n$ )	$M_{n,NMR}^d$ PEG-polyesters	$M_w/M_n^c$
1a-MPEG-b-PCL	17.5	2000–2000	98 <sup>b1</sup>	3870	2000–2060	1.14
2a-PCL-b-PEG-b-PCL	17.5	2000–2000	98 <sup>b1</sup>	3730	2000–2100	1.24
4a-PEG-b-PCL	17.5	2000–2000	99 <sup>b1</sup>	2410	2000–2060	1.22
8a-PEG-b-PCL	17.5	2000–2000	99 <sup>b1</sup>	1450	2000–2090	1.31
4a-PEG-b-PDO	28	2000–2000	90 <sup>b2</sup>	1740	2000–1990	1.41
4a-PEG-b-PTMC	19.6	2000–2000	97 <sup>b3</sup>	1960	2000–2100	1.28
4a-PEG-b-PLGA <sup>e</sup>	6.9/8.6	2000–1000/1000	91 <sup>b4</sup>	1970	2000–1900	1.33

Condition: [HCl]/[Initiator] = 2, [Monomer]/[CH<sub>2</sub>Cl<sub>2</sub>] = 0.5 M, room temperature, 24 h.

<sup>a</sup> MPEG = 2000 ( $M_w/M_n$  = 1.08), PEG = 2000 ( $M_w/M_n$  = 1.09), four-arm-PEG = 2000 ( $M_w/M_n$  = 1.10), eight-arm-PEG = 2000 ( $M_w/M_n$  = 1.14).

<sup>b</sup> <sup>b1</sup> *n*-Hexane insoluble part, <sup>b2</sup> Ether/heptane (4/1) insoluble part, <sup>b3</sup> Methanol insoluble part, <sup>b4</sup> *n*-Hexane/ether (4/1) insoluble part.

<sup>c</sup> Measured by gel permeation chromatography (based on standard polystyrene).

<sup>d</sup> Determined by <sup>1</sup>H NMR.

<sup>e</sup> [Sn(Oct)<sub>2</sub>]/[initiator] = 0.6, [LA + GA]/[toluene] = 1 M, 130 °C, 24 h. [LA]/[GA] = 5/5 (mole ratio).

ester main chain (ethylene oxide units/ester units). The molecular weight values calculated in this manner are in excellent agreement with the theoretical values ([2000]/[2000] g/mol) calculated from the PEG/polyester ratio employed (Table 1). These findings indicate that in the polymerization using HCl Et<sub>2</sub>O as a monomer activator, the molecular weight of the polyester segment can be controlled well by varying the [PEG core]/[ester monomer] ratio.

Figure 2 shows the GPC curves of (a) PEG precursor and (b) PEG-*b*-PCL star block copolymers with one, two, four, or eight arms. The entire GPC curve shifts to shorter retention times after the polymerization compared with the curve for the PEG precursor. The monomodal nature of all of the GPC curves, which show no traces of low molecular weight material, indicates that the homopolymerization of polyester occurred to a negligible degree. These findings imply that all of the PEG core was incorporated into the star polymer and all of the PEG hydroxyl groups acted as initiators to give the star block polymer.

The GPC-determined number-average molecular weights ( $M_{n,GPC}$ ) of these star block polymers were smaller than the corresponding NMR-determined number-average molecular weights ( $M_{n,NMR}$ ),<sup>34</sup> a discrepancy that increased as the arm number increased. In addition, the molecular weight distribution ( $M_w/M_n$ ) of the star polymers broadened slightly as the arm number increased. The discrepancy between  $M_{n,GPC}$  and  $M_{n,NMR}$  was likely due to both the

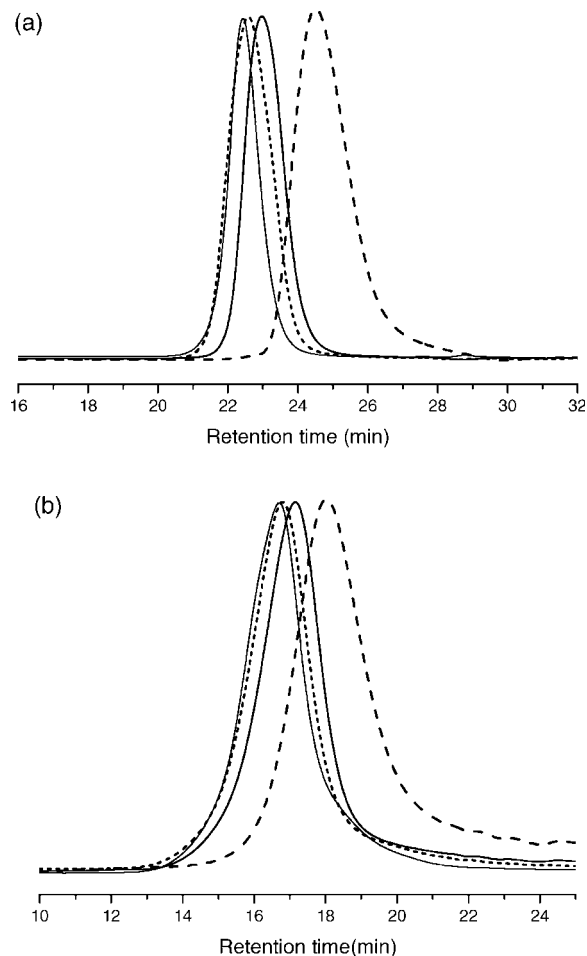


**Figure 2.** GPC curves of (a) PEG precursor and (b) PEG-*b*-PCL star block copolymers with one arm (plain line), two arms (short dash line), four arms (bold line), and eight arms (dash line).

**Table 2.** The Thermal Properties and Degree of Crystallinity for PEG-*b*-polyester Star Block Copolymers

Sample	PEG Block <sup>a</sup>		Polyester Block <sup>a</sup>		$\chi_c^b$
	$T_m$ (°C)	$\Delta H_m$ (J/g)	$T_m$ (°C)	$\Delta H_m$ (J/g)	
1a-MPEG- <i>b</i> -PCL	19.2	3	49.3	138	44.1
2a-PCL- <i>b</i> -PEG- <i>b</i> -PCL	19.6	6	40.1	101	39.7
4a-PEG- <i>b</i> -PCL	14.4	57	31.3	34	21.1
8a-PEG- <i>b</i> -PCL	14.1	54	20.6	10	10.7
4a-PEG- <i>b</i> -PDO	–	–	69	48	14.5
4a-PEG- <i>b</i> -PTMC	–	–	–	–	–
4a-PEG- <i>b</i> -PLGA	–	–	–	–	–

<sup>a</sup> Measured by DSC.

<sup>b</sup>  $\chi_c$  was calculated as the ratio of the crystalline peak areas to the total areas under the scattering curve.

constrained geometry and the molecular interactions among the PEG-*b*-polyester star block copolymers, which resulted in a smaller hydrodynamic volume. Therefore, GPC measurements carried out in CHCl<sub>3</sub> with polystyrene calibration lead to grossly underestimated values due to the structure of PEG-*b*-polyester star block copolymers, which becomes increasingly compact with increasing arm number.

The 4a-PEG-*b*-PDO and 4a-PEG-*b*-PTMC star block polymers synthesized by polymerization using HCl Et<sub>2</sub>O as a monomer activator were also obtained in quantitative yield, and showed PEG and polyester segment contents in excellent agreement with the theoretical values. Thus, PEG-*b*-polyester star block copolymers could be successfully prepared via a metal-free method using HCl Et<sub>2</sub>O as the monomer activator.

### Crystallinity of PEG-*b*-polyester Star Block Copolymers

The crystallinity characteristics of the PEG-*b*-polyester star block copolymers were investigated using differential scanning calorimetry (DSC) and X-ray diffraction (XRD) in the bulk state, as summarized in Table 2. In the DSC thermograms, two peaks, assigned to the crystallization of the PEG and PCL segments of the star block copolymers, were clearly visible. These peaks shifted to lower temperature as the arm number increased from one to eight arms. However, the melting enthalpies for the PEG block increased with increasing arm number, whereas those of the PCL block decreased. This

may indicate that the PEG in the core of the star copolymer crystallizes more readily than linear PEG, with the tendency to crystallize increasing with increasing arm number. The decrease in melting enthalpy of the PCL block with increasing arm number suggests that, as the number of arms in the star block copolymer increases, the PCL outer block becomes more mobile and hence crystallization of this block becomes more difficult. XRD analysis of the star block copolymers indicated that their crystallinity decreased from 44 to 11% as the arm number increased from 1 to 8. Therefore, the PCL and PEG blocks strongly influenced each other. These findings indicate that the crystalline properties of the star block copolymers can be controlled by varying the arm number.

Compared with the PEG-*b*-PCL star block copolymers, 4a-PEG-*b*-PDO showed a lower degree of crystallinity. Only one peak was observed in the DSC thermogram, at 69 °C, which was assigned to the melting point of the PDO blocks.<sup>35</sup> The different crystallization characteristics of this star block copolymer may be due to the ether group in the PDO segments having a synergistic influence on the segmental mobility, leading to a lowering of the crystallization enthalpy of the PEG block segments, likely due to phase mixing between PEG and PDO blocks.<sup>36</sup>

In the DSC thermograms for 4a-PEG-*b*-PTMC and 4a-PEG-*b*-PLGA, no peaks were observed corresponding to the melting points of PEG and PTMC or PLGA, since PTMC and PLGA are amorphous polymer. Moreover, the XRD patterns for these star block copolymers were characteristic of an amorphous structure, indicating

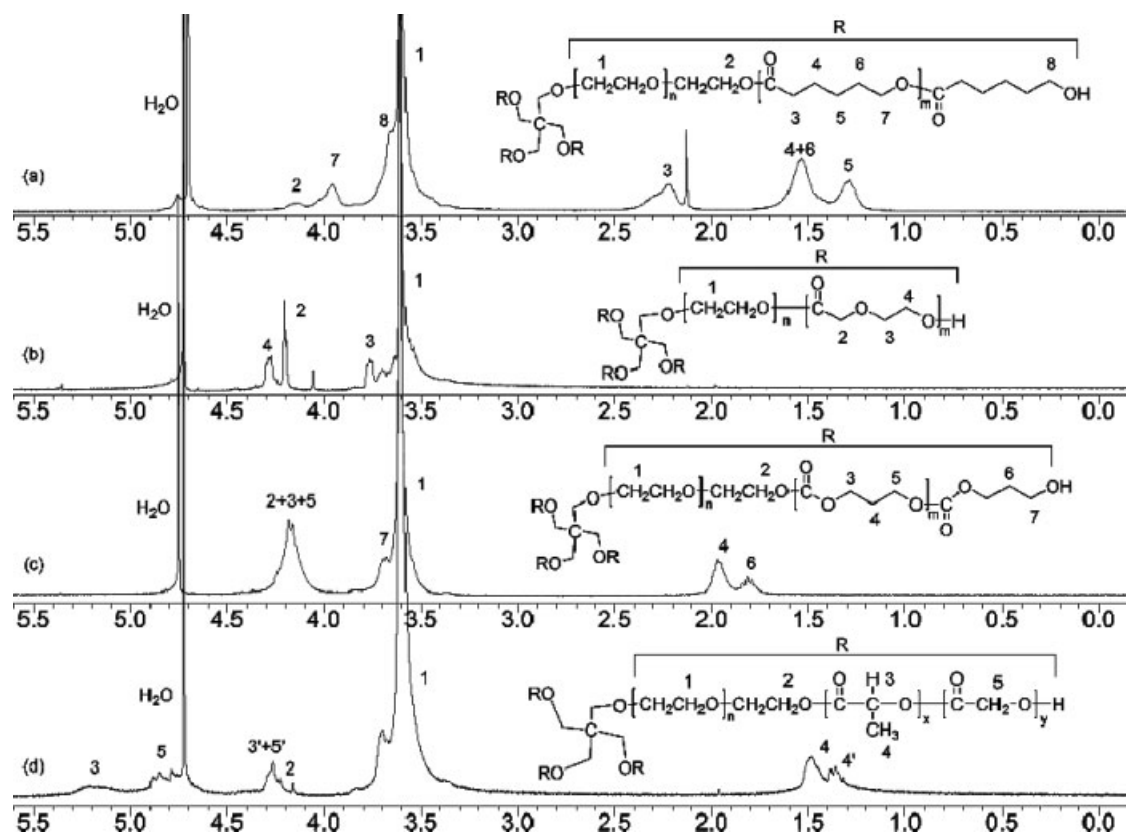


**Figure 3.**  $^1\text{H}$  NMR spectra of various four-arm PEG-*b*-polyester star block copolymers in  $\text{D}_2\text{O}$ : (a) 4a-PEG-*b*-PCL, (b) 4a-PEG-*b*-PDO, (c) 4a-PEG-*b*-PTMC, and (d) 4a-PEG-*b*-PLGA.

that these materials do not crystallize. The observed behavior is consistent with the PTMC and PLGA blocks remaining amorphous at all temperatures, and the disordered structures of these blocks restricting the crystallization of the core PEG block. These findings therefore indicate that PEG-*b*-polyester star block copolymers with different crystallinities can be designed by adjusting the nature of the polyester segments (PCL, PDO, PTMC, or PLGA). Taken together, the present results indicate that the crystallinity of the star block copolymers synthesized in this work depended on both the nature of the polyester block segment as well as the number of arms.

### Study of Micelles

When added to an aqueous phase, amphiphilic block copolymers form micelles with a core-shell structure. Figure 3 shows the  $^1\text{H}$  NMR spectra for various four-arm star block copolymers at 1 wt % concentration in  $\text{D}_2\text{O}$  at room temperature. Compared with the spectra of these copolymers in  $\text{CDCl}_3$  (Fig. 1), which showed clear resonance

peaks arising from both the PEG and polyester blocks, the peaks arising from the polyester blocks are broader in the  $\text{D}_2\text{O}$  spectra. This indicates that in  $\text{D}_2\text{O}$ , the molecular motion of the polyester blocks is limited, whereas that of the PEG blocks is not, consistent with the preferential localization of the polyester blocks inside the micellar core and the PEG blocks at the outer shell of the micelles adjoining the aqueous phase. The  $^1\text{H}$  NMR spectral data thus indicate that in aqueous media, the PEG-*b*-polyester star block copolymers studied herein form a micelles in which the hydrophobic outer arms are encapsulated by the hydrophilic core.

The CMC of the resulting micellar system will depend on various characteristics of the amphiphilic block copolymer, including the nature and length of the core forming block, the lengths of the hydrophilic and hydrophobic blocks, and the structural architecture of the block copolymer. Thus the CMC investigation is important for determining whether the PEG-*b*-polyester star block copolymers can be considered as potential drug carriers.

**Table 3.** CMC and  $K_v$  Determined by PEG-*b*-polyester Star Block Copolymers

Sample	CMC $\times 10^3$ (mg/mL)	$K_v \times 10^{-4}$
1a-MPEG- <i>b</i> -PCL	1.26	16.0
2a-PCL- <i>b</i> -PEG- <i>b</i> -PCL	2.51	10.7
4a-PEG- <i>b</i> -PCL	3.98	8.6
8a-PEG- <i>b</i> -PCL	5.62	5.9
4a-PEG- <i>b</i> -PDO	7.08	2.0
4a-PEG- <i>b</i> -PTMC	18.8	1.5
4a-PEG- <i>b</i> -PLGA	10.2	1.9

As described in the previous section, we successfully prepared PEG-*b*-polyester star block copolymers whose hydrophobic and hydrophilic segments had similar molecular weights. The amphiphilic nature of the segments of these star block copolymers means that they can form micelles in aqueous media. Thus, we examined the micelle formation characteristics of the PEG-*b*-polyester star block copolymers in deionized water.

Fluorescence measurements using pyrene as a probe were carried out to determine the CMCs of the various star block copolymers in aqueous solution at room temperature. Pyrene, a hydrophobic molecule, is preferentially localized inside or close to the hydrophobic microdomain of micelles; hence the photophysical characteristics of pyrene in micelles are different from those of free pyrene molecules in water. The pyrene excitation spectrum shifted from 335 nm for free pyrene to 338 nm for the micellar system, indicating partitioning of pyrene into the hydrophobic micellar core. This shift was utilized to determine the CMC values. The fluorescence intensity ratio ( $I_{338}/I_{335}$ ) of pyrene excitation spectra was plotted against the logarithm of the concentration of the PEG-*b*-polyester star block copolymer. A substantial increase of the intensity ratio begins at a certain concentration, indicating the onset of micelle formation. The intercept of straight line fits of the intensity ratio data above and below this onset point is taken as the CMC.

The CMCs determined from the fluorescence measurements are listed in Table 3. The CMCs of PEG-*b*-PCL star block copolymers increase with increasing arm number, suggesting that block copolymers with star architectures may be less amenable to micellization than the corresponding linear block copolymers. This is attributed to decreased aggregation of the hydropho-

bic segments with increasing arm number. Another reason may be the architecture of the star block copolymers. In aqueous solution, the aggregation of the outer PCL blocks with short length is hindered by the lower mobility of the PCL outer blocks exposed to the surrounding water. This hindering of PCL aggregation can be understood in terms of the translational entropic change associated with the formation of micellar aggregates, which increases with increasing arm number. Consequently, the CMC increases as the arm number increases.

For the four-arm star block copolymers with different polyester segments, the CMC increased in the following order: 4a-PEG-*b*-PCL < 4a-PEG-*b*-PDO < 4a-PEG-*b*-PLGA < 4a-PEG-*b*-PTMC. This sequence indicates that the star block copolymers with more crystalline segments formed micelles more easily than those with lower crystallinity. These findings thus suggest that as the crystallinity of the domains of polyester blocks decreases, the interactions between the hydrophobic blocks in the block copolymer become weaker.

Figure 4 shows pictures of various star block copolymers at 1 wt % concentration in deionized water at room temperature. The turbidity of the solution indicates the degree of aggregation of the star block copolymers into micelles. Inspection of the solutions reveals that the turbidity increases with increasing arm number, while the solution of 4a-PEG-*b*-PLGA or 4a-PEG-*b*-PTMC, which has amorphous segments, is clear. The mean hydrodynamic diameters of the micelles, as determined from dynamic light scattering measurements, also increased from 150 to 860 nm with increasing arm number (Fig. 5). This change in mean hydrodynamic diameter arises from the micelle structure, where the decreasing length of the hydrophobic segments with increasing arm number restricts aggregation.

To explore the morphologies of the aggregates, we used atomic force microscopy (AFM) to examine the micelles of the star block copolymers at 1 wt % concentration in water. Figure 6 shows AFM images of the micelles formed in deionized water by PEG-*b*-PCL star block copolymers with different arm numbers. The AFM images revealed that most of the micelles were spherical, with nonspherical micelles being observed only rarely. The diameters of the micelles observed by AFM were in good agreement with the values determined from DLS observations.

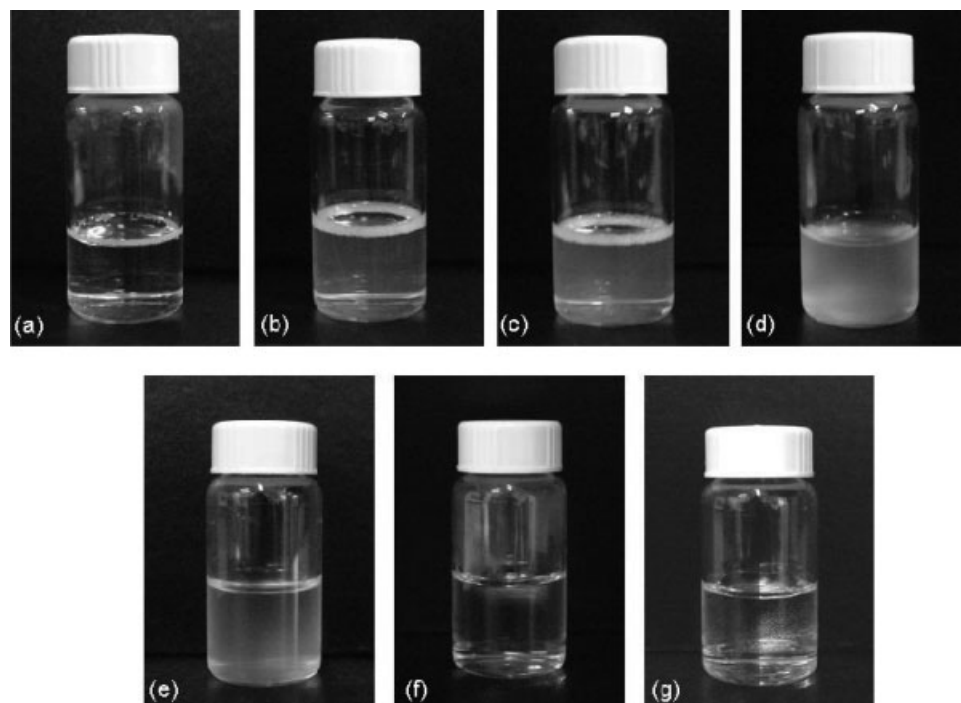


**Figure 4.** Images of the micelle solutions formed from PEG-*b*-PCL star block copolymers with (a) one arm, (b) two arms, (c) four arms, and (d) eight arms, as well as (e) 4a-PEG-*b*-PDO, (f) 4a-PEG-*b*-PTMC, and (g) 4a-PEG-*b*-PLGA.

#### Partitioning of Pyrene to the Micellar Core

The method of Wilhelm et al.<sup>37</sup> can be used to calculate the partition equilibrium constant,  $K_v$ , characteristic of the hydrophobicity of the micellar core for PEG-*b*-polyester star block copolymers. The  $K_v$  of pyrene was calculated by considering the incorporation of pyrene into the micelles as a simple equilibrium between the micellar phase ( $[\text{Py}]_m$ ) and the aqueous phase ( $[\text{Py}]_w$ ). Thus, the ratio of pyrene concentration in the micellar to the aqueous phase ( $[\text{Py}]_m/[\text{Py}]_w$ ) can be correlated to the volume ratio of each phase according to:

$$[\text{Py}]_m/[\text{Py}]_w = K_v V_m/V_w \quad (1)$$

which can be rewritten as

$$[\text{Py}]_m/[\text{Py}]_w = K_v x \times (c - \text{CMC})/1000\rho \quad (2)$$

where  $x$  is the weight fraction of hydrophobic polyester block,  $c$  is the concentration of the block copolymer, and  $\rho$  is the density of the polyester micellar core, which is assumed to be equal to the value for bulk PCL (1.15),<sup>38</sup> PDO (1.38),<sup>39,40</sup> PLGA (1.30),<sup>41</sup> or PTMC (1.01).<sup>42</sup>

$[\text{Py}]_m/[\text{Py}]_w$  can be written as

$$[\text{Py}]_m/[\text{Py}]_w = (F - F_{\min})/(F_{\max} - F) \quad (3)$$

where  $F_{\min}$  and  $F_{\max}$  correspond to the average magnitude of  $I_{338}/I_{335}$  in the flat region of low and high concentration ranges and  $F$  is the  $I_{338}/I_{335}$  intensity ratio in the intermediate concentration range of the block copolymers. By combining eqs. 2 and 3,  $K_v$  was determined from the slope of a plot of  $(F - F_{\min})/(F_{\max} - F)$  versus block copolymer concentration at concentrations above the CMC (Fig. 7).  $K_v$  may be an indicator of the hydrophobicity of the PEG-*b*-polyester star block copolymers.

The  $K_v$  values for the PEG-*b*-polyester star block copolymers are summarized in Table 3. For PEG-*b*-PCL star block copolymers with different arm numbers,  $K_v$  decreases in the order: 1a-PEG-*b*-PCL > 2a-PCL-*b*-PEG-*b*-PCL > 4a-PEG-*b*-PCL > 8a-PEG-*b*-PCL. The  $K_v$  values ranged from  $1.6 \times 10^5$  to  $5.9 \times 10^4$ , in the opposite order to the CMCs. As the arm number of the hydrophobic block of the copolymers increases, the  $K_v$  value decreases, suggesting that the hydrophobicities of the micellar core also decrease. These findings indicate that the



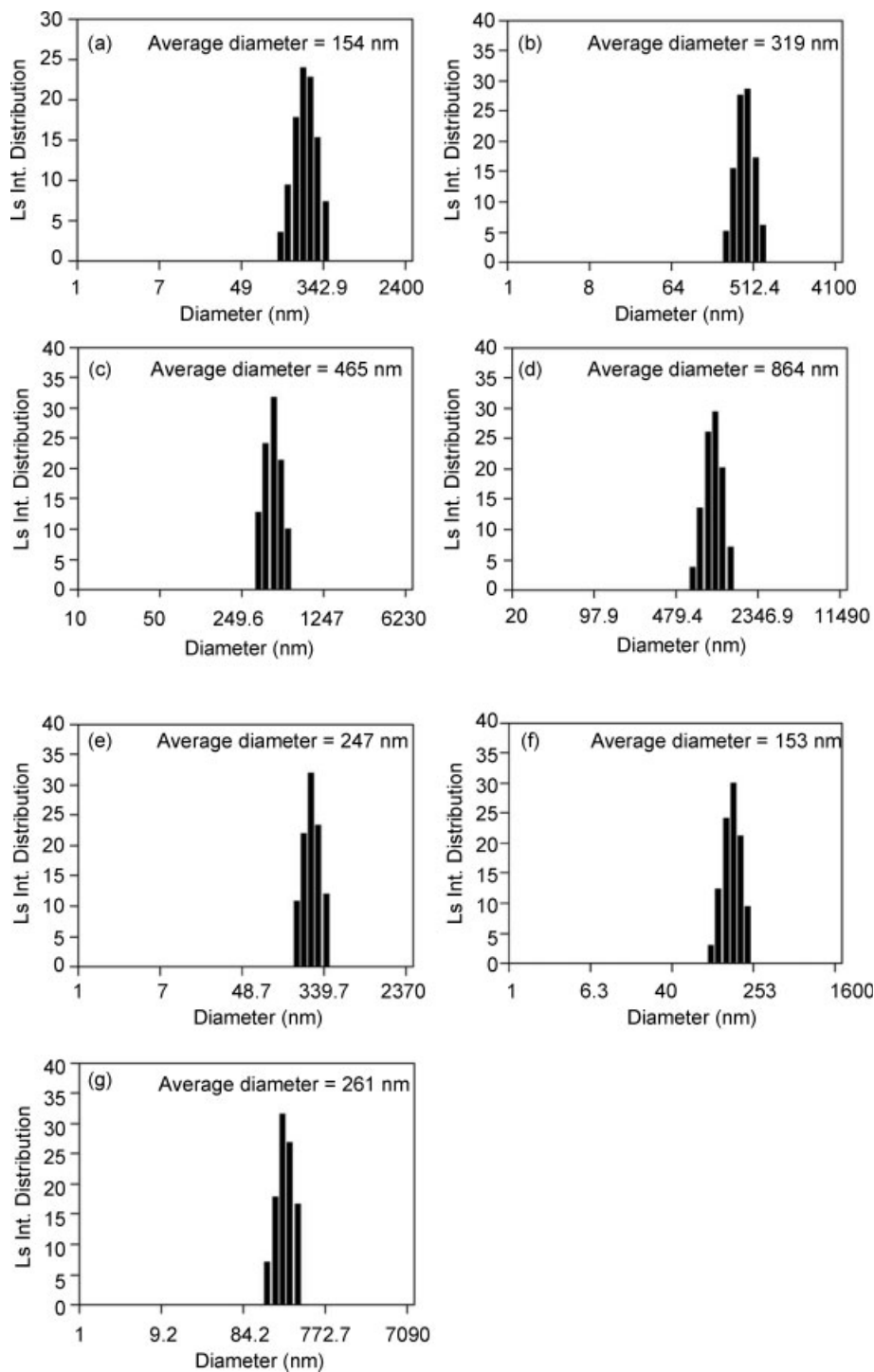


**Figure 5.** The micelle size distribution of PEG-*b*-PCL star block copolymers: (a) one arm, (b) two arms, (c) four arms, and (d) eight arms, as well as (e) 4a-PEG-*b*-PDO, (f) 4a-PEG-*b*-PTMC and (g) 4a-PEG-*b*-PLGA.

capacity of hydrophobic parts of the star block copolymers to be solubilized in micelles diminishes as the arm number increases and the crystallinity decreases.

For the four-arm copolymers, 4a-PEG-*b*-PCL, 4a-PEG-*b*-PDO, 4a-PEG-*b*-PTMC, and 4a-PEG-*b*-PLGA, we obtained  $K_V$  values of  $8.6 \times 10^4$ ,  $2.0 \times 10^4$ ,  $1.5 \times 10^4$ , and  $1.9 \times 10^4$ , respectively.

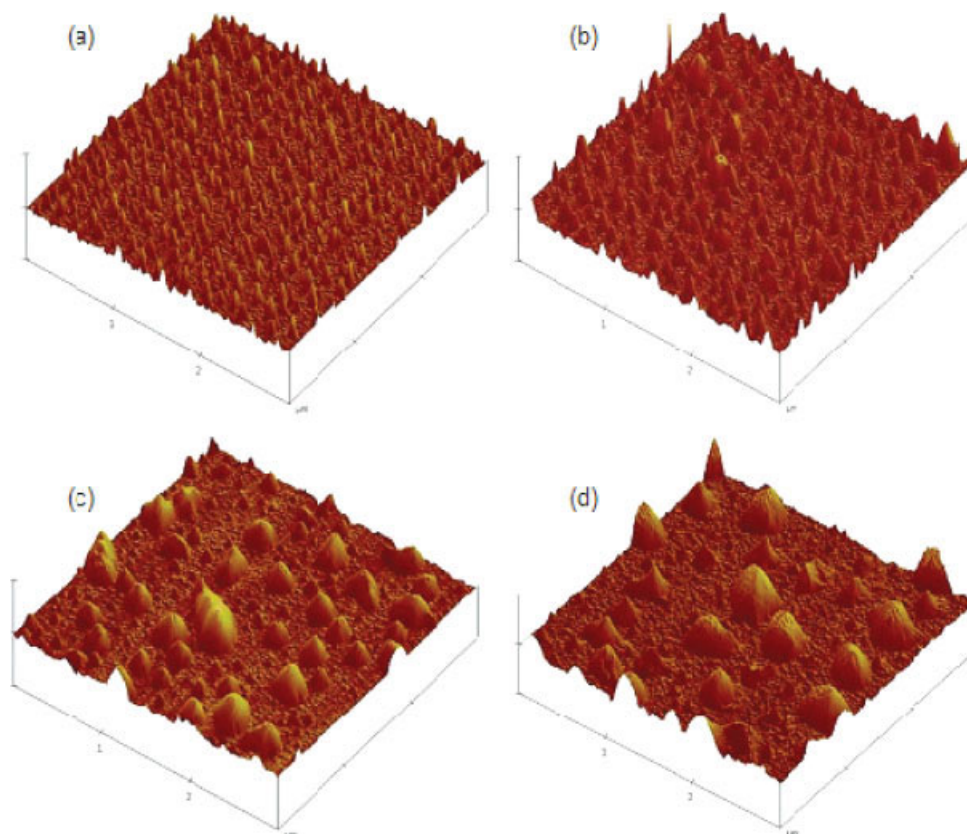


**Figure 6.** AFM three-dimensional images ( $3 \times 3 \mu\text{m}^2$ ) of micelles prepared from PEG-*b*-PCL star block copolymers with (a) one arm, (b) two arms, (c) four arms, and (d) eight arms. Z-scale is (a–c) 50 nm and (d) 100 nm.

Notably, the partition coefficient for pyrene in 4a-PEG-*b*-PCL micelles was approximately four-fold higher than those of the four-arm star block copolymers with other polyester blocks. These findings indicate that the partition coefficient for pyrene is higher in star block copolymers with more crystalline domains. The observation of a higher partition coefficient for 4a-PEG-*b*-PCL than for the other four-arm star block copolymers suggests that pyrene is more easily trapped in the hydrophobic regions of 4a-PEG-*b*-PCL, likely because the higher crystallinity of this star block copolymer enhances the hydrophobicity of the cores of micelles formed from this copolymer, thereby making the core a more attractive environment for pyrene.

## CONCLUSIONS

We prepared various PEG-*b*-polyester star block copolymers via ROP of CL, TMC, or DO initi-

ated at the hydroxyl end group of core PEG in the presence of HCl Et<sub>2</sub>O as a monomer activator. These polymerization reactions afforded large quantities of the PEG-*b*-polyester star block copolymers in quantitative yield, without residual products. The PEG-*b*-polyester star block copolymers had molecular weights close to the theoretical values calculated from the molar ratio of ester monomers to PEG, and exhibited monomodal GPC curves. This polymerization procedure yielded PEG-*b*-polyester star block copolymers with well-defined structures by a metal-free method.

The crystallinity of the PEG-*b*-polyester star block copolymers depended on the arm number as well as the nature of the polyester block. In addition, the CMC of the PEG-*b*-PCL star block copolymers increased as the arm number increased. Moreover, among the four-arm star block copolymers with different polyester segments, the CMC increased with increasing crystallinity of the star block copolymer. The partition

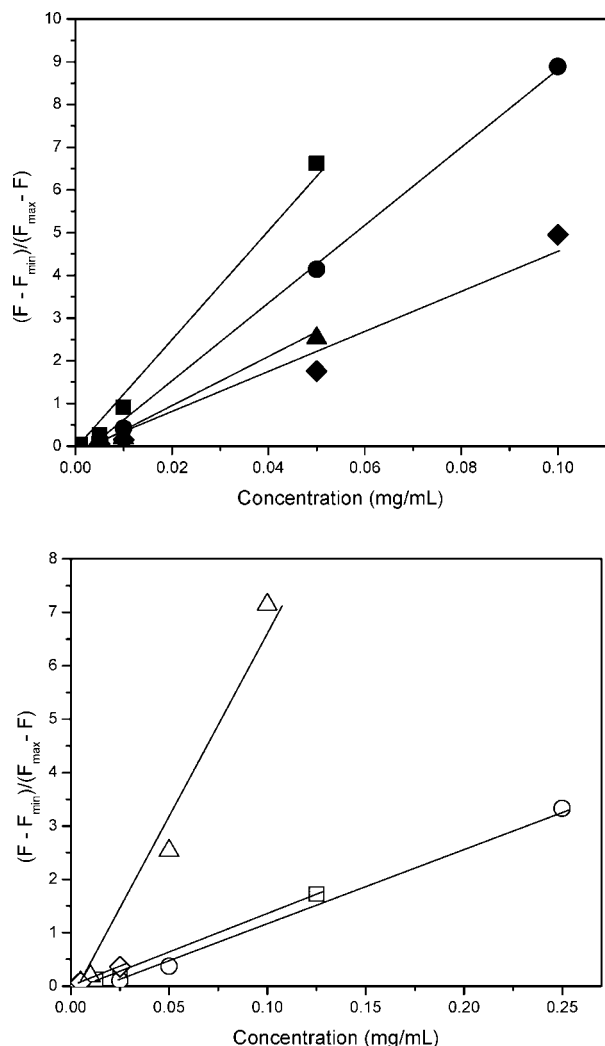


**Figure 7.** Plots of  $(F - F_{\min})/(F_{\max} - F)$  versus concentration of block copolymers at 25 °C; (■) 1a-PEG-*b*-PCL, (●) 2a-PCL-*b*-PEG-*b*-PCL, (▲) 4a-PEG-*b*-PCL, (◆) 8a-PEG-*b*-PCL, (△) 4a-PEG-*b*-PCL, (□) 4a-PEG-*b*-PDO, (○) 4a-PEG-*b*-PTMC, and (◇) 4a-PEG-*b*-PLGA.

equilibrium constant,  $K_v$ , also depended on the arm number and the crystallinity of the star block copolymers.

The PEG-*b*-polyester star block copolymers prepared in this work are candidate materials for use as hydrophobic drug delivery vehicles, and do not contain the undesirable metal contaminants typically found in copolymers obtained by conventional ROP with a metal initiator. In ongoing studies, we are investigating the biomedical application of hydrophobic-drug-loaded micelles prepared using PEG-*b*-polyester star block copolymers.

## EXPERIMENTAL

### Materials

MPEG ( $M_n = 2000$ , Aldrich), PEG with two terminal alcohols ( $M_n = 2000$ , Aldrich), PEG with four terminal alcohols ( $M_n = 2000$ , NOF), PEG with eight terminal alcohols ( $M_n = 2000$ , NOF), and HCl (1.0 M solution in diethyl ether, Aldrich) were used as received. CL was distilled over  $\text{CaH}_2$  under reduced pressure. TMC (Boehringer Ingelheim, Germany) was recrystallized in xylene. 1,4-Dioxane-2-one (DO, Metabio, Korea) was used as received. LA (Boehringer Ingelheim, Germany) and GA (Boehringer Ingelheim, Germany) were recrystallized in ethyl acetate two times.  $\text{CH}_2\text{Cl}_2$  was distilled sequentially from  $\text{CaCl}_2$  and  $\text{CaH}_2$  under nitrogen before use.

### Instrumentation

$^1\text{H}$  NMR spectra were measured using Bruker 300 instrument with  $\text{CDCl}_3$  in the presence of tetramethylsilane as internal standard or with  $\text{D}_2\text{O}$ . Molecular weights and molecular weight distributions of PEG and PEG-*b*-polyester star block copolymers were estimated by gel permeation chromatography (GPC) on Futecs At-3000 GPC system (Shodex RI-71 detector) using two columns (Shodex K-802 polystyrene gel column and Shodex Asahipak GF-510 HQ polyvinyl alcohol gel column) at 45 °C, using  $\text{CHCl}_3$  as an eluent with a flow rate of 0.8 mL/min by polystyrene calibration.

### Synthesis of Four-Arm-Poly(ethylene glycol)-*block*-poly( $\epsilon$ -caprolactone) Star Block Copolymers (4a-PEG-*b*-PCL)

All glasses were dried by heating in vacuum and handled under a dry nitrogen stream. The typical process for the polymerization to give 4a-PEG-*b*-PCL is as follows. 4a-PEG ( $M_n = 2000$ ) (1.5 g, 0.75 mmol) and toluene (80 mL) were introduced into a flask. The 4a-PEG solution was distilled by azeotropic distillation to remove water. Toluene was then distilled off completely. To 4a-PEG was added the  $\text{CH}_2\text{Cl}_2$  (20 mL), followed by the addition of CL (1.5 g, 13 mmol). The polymerization was initiated by the addition of 1.0 M solution of HCl in diethyl ether (1.5 mL, 1.5 mmol) at 25 °C. After 24 h, the reaction mixture was poured into methanol

to precipitate a polymer, which was separated from the supernatant by decantation. The obtained polymer was redissolved in  $\text{CH}_2\text{Cl}_2$  and then filtered. The polymer solution was concentrated by rotary evaporator and dried in vacuum to give a colorless polymer of quantitative yield. The TMC monomer conversion was determined by  $^1\text{H}$  NMR spectroscopy before precipitation with methanol. The molecular weight of PCL segment in the block copolymer was determined by the intensity of methylene proton signal of 4a-PEG at  $\delta = 3.64$  ppm and methylene proton signal of PCL at  $\delta = 2.31$  ppm in  $^1\text{H}$  NMR spectroscopy.

#### Determination of Critical Micelle Concentration

The CMC was determined using pyrene as a fluorescence probe. One milliliter of pyrene solution in THF (1.2 mM) was added to 1000 mL of distilled water. THF was removed by a rotary evaporator at 30 °C for 2 h to give pyrene solution in water ( $1.2 \times 10^{-6}$  M). Stock solutions of star block copolymer were prepared by dissolving the star block copolymer samples in distilled water under stirring. From the stock solution, a series of concentration was prepared by dilution. The pyrene solution was added by the star block copolymer solution. The solutions after filtration using 0.45  $\mu\text{m}$  membrane filter were allowed to stand overnight at room temperature to equilibrate. The formed micelle sizes were measured by electrophoretic light scattering (ELS-8000, Photal, Otsuka Electronics, Tokyo, Japan). The micelle concentration in these experiments varied from  $0.5 \times 10^{-7}$  to 1.0 mg/mL. The pyrene concentration in star block copolymer solution was  $6 \times 10^{-7}$  M. For the measurements of pyrene excitation spectra scan speed was set at 240 nm/min and, emission and excitation slit widths were set at 2.5 nm. For the excitation spectra, the emission wavelength was 373 nm. Fluorescence intensities of the pyrene entrapped in the micelle core were determined by an F-4500 fluorescence spectrophotometer ( $I_{\text{ex}}$  338 nm, Hitachi Co. LTD, Japan) at room temperature.

#### Atomic Force Microscopy

One drop of star block copolymer solution was transferred onto silicone wafer, which is washed with MeOH. The wafer was quickly placed in liquid nitrogen, followed by the freeze-drying for

3 days. AFM measurements were carried out in the tapping mode with a Nanoscope IV instrument (Digital Instruments Inc.).

This work was supported by a grant from KMOHW (grant no A050082).

#### REFERENCES AND NOTES

1. Yagci, Y.; Tasdelen M. A. *Prog Polym Sci* 2006, 31, 1133.
2. Zhao, Y.; Higashihara, T.; Sugiyama, K.; Hirao, A. *Macromolecules* 2007, 40, 228.
3. Lorenzo, A. T.; Müller, A.; Priftis, J. D.; Pitsikalis, M.; Hadjichristidis, N. *J Polym Sci Part A: Polym Chem* 2007, 45, 5387.
4. Kreutzer, G.; Ternat, C.; Nguyen, T. Q.; Plummer, C. J. G.; Manson, J.-A. E.; Castelletto, V.; Hamley, I. W.; Sun, F.; Sheiko, S. S.; Herrmann, A.; Ouali, L.; Sommer, H.; Fieber, W.; Velazco, M. I.; Klok, H.-A. *Macromolecules* 2006, 39, 4507.
5. Lapienis, G. *J Polym Sci Part A: Polym Chem* 2007, 45, 5017.
6. Saito, N.; Murakami, N.; Takahashi, J.; Horiuchi, H.; Ota, H.; Kato, H.; Okada, T.; Nozaki, K.; Takaoka, K. *Adv Drug Deliv Rev* 2005, 57, 1037.
7. Dhanikula, R. S.; Hildgen, P. *Bioconjugate Chem* 2006, 17, 29.
8. Vakil, R.; Kwon, G. S. *Langmuir* 2006, 22, 9723.
9. Li, X.; Liu, K. L.; Li, J.; Tan, E. P. S.; Chan, L. M.; Lim, C. T.; Goh, S. H. *Biomacromolecules* 2006, 7, 3112.
10. Smeenk, J. M.; Schon, P.; Otten, M. B. J.; Speller, S.; Stunnenberg, H. G.; van Hest, J. C. M. *Macromolecules* 2006, 39, 2989.
11. He, C.; Sun, J.; Zhao, T.; Hong, Z.; Zhuang, X.; Chen, X.; Jing, X. *Biomacromolecules* 2006, 7, 252.
12. Kricheldorf, H. R.; Rost, S.; Wutz, C.; Domb, A. *Macromolecules* 2005, 38, 7018.
13. Discher, D. E.; Ortiz, V.; Srinivas, G.; Klein, M. L.; Kim, Y.; Christian, D.; Cai, S.; Photos, P.; Ahmed, F. *Prog Polym Sci* 2007, 320, 838.
14. Sung, G. A.; Guang, H. L.; Chang, G. C. *Polymer* 2006, 47, 4154.
15. Bogdanov, B.; Vidts, A.; Buicke, A.; Verbeeck, R.; Schacht, E. *Polymer* 1998, 39, 1631.
16. Morinaga, H.; Ochiai, B.; Endo T. *J Polym Sci Part A: Polym Chem* 2006, 44, 6633.
17. Pang, K.; Kotek, R.; Tonelli, A. *Prog Polym Sci* 2006, 31, 949.
18. Cai, C.; Wang, L.; Dong, C. M. *J Polym Sci Part A: Polym Chem*, 2006, 44, 2034.
19. Hiemstra, C.; Zhong, Z.; Li, L.; Dijkstra, P. J.; Feijen, J. *Biomacromolecules* 2006, 7, 2790.
20. Lemmouchi, Y.; Perry, M. C.; Amass, A. J.; Chakraborty, K.; Schacht, E. *J Polym Sci Part A: Polym Chem* 2007, 45, 3975.

21. Lemmouchi, Y.; Perry, M. C.; Amass, A. J.; Chakraborty, K.; Schacht, E. J. *J Polym Sci Part A: Polym Chem* 2007, 45, 3966.
22. Remant, B.; Shanta, R. B.; Santosh, A.; Khil, M. S.; Dharmaraj, N.; Kim, H. Y. *Colloids Surfaces A: Physicochem Eng Aspects* 2007, 292, 69.
23. Kim, M. S.; Hyun, H.; Khang, G.; Lee, H. B. *Macromolecules* 2006, 39, 3099.
24. Hyun, H.; Kim, M. S.; Khang, G.; Lee, H. B. *J Polym Sci Part A: Polym Chem* 2006, 44, 4235.
25. Morinaga, H.; Ochiai, B.; Mori, H.; Endo, T. *J Polym Sci Part A: Polym Chem*, 2006, 44, 1985.
26. Pitt, C. G.; Schindler, A.; Zatushni, G. L.; Goldsmith, A.; Shelton, J. D.; Sciarra, J. J. *Long-Acting Contraceptive Delivery Systems*, Harper-collins College Division, Northwestern University, 1984, 48.
27. Myers, M.; Connor, E. F.; Glauser, T.; Mock, A.; Nyce, G.; Hedrick, J. L. *J Polym Sci Part A: Polym Chem* 2002, 40, 844.
28. Wilson, B. C.; Jones, C. W. *Macromolecules* 2004, 37, 9709.
29. Kim, M. S.; Seo, K. S.; Khang, G.; Lee, H. B. *Macromol Rapid Commun* 2005, 26, 643.
30. Kim, M. S.; Kim, S. K.; Kim, S. H.; Hyun, H.; Khang, G.; Lee, H. B. *Tissue Eng* 2006, 12, 2863.
31. Lee, S. J.; Han, B. R.; Park, S. Y.; Han, D. K.; Kim, S. C. *J Polym Sci Part A: Polym Chem* 2006, 44, 888.
32. Shibasaki, Y.; Sanda, F.; Endo, T. *Macromol Rapid Commun* 1999, 20, 532.
33. Shibasaki, Y.; Sanada, H.; Yokoi, M.; Sanda, F.; Endo, T. *Macromolecules* 2000, 33, 4316.
34. One referee pointed out that the actual molecular weights of aliphatic polyesters are considerably lower than that determined with polystyrene calibration (Save, M.; Schappacher, M.; Soum, A.; *Macromol Chem Phys* 2002, 203, 889). However, we suppose that the difference in the GPC column (polystyrene/polyvinyl alcohol gel columns and polystyrene only) and type of polymer (PEG-polyester block copolymers and aliphatic polyesters) resulted in different results.
35. Bhattarai, N.; Kim, H. Y.; Lee, D. R.; Park, S. J. *Polym Int* 2003, 52, 6.
36. Kricheldorf, H. R.; Damrau, D. O. *Macromol Chem Phys* 1998, 199, 1089.
37. Wilhelm, M.; Zhao, C.; Wang, Y.; Xu, R.; Winnik, M. A.; Mura, J.; Riess, G.; Croucher, M. D. *Macromolecules* 1991, 24, 1033.
38. Lee, S. C.; Chang, Y.; Yoon, J. S.; Kim, C.; Kwon, I. C.; Kim, Y. H.; Jeong, S. Y. *Macromolecules* 1999, 32, 1847.
39. Haruo, N.; Mitsuhiro, Y.; Takeshi, E.; Yutaka, T. *Macromolecules* 2000, 33, 6982.
40. Gertzman, A.; Thompson, D. R. Annealed polydioxanone surgical device and method for producing the same, U.S. patent 4,591,630.
41. Kim, C.; Lee, S. C.; Shin, J. H.; Yoon, J. S.; Kwon, I. C.; Jeong, S. Y. *Macromolecules* 2000, 33, 7448.
42. Doneva, T. A.; Yin, H. B.; Stephens, P.; Bowen, W. R.; Thomas, D. W. *Spectroscopy* 2004, 18, 587.